First-principles pseudopotential calculations for hydrogen in 4d transition metals. II. Vibrational states for interstitial hydrogen isotopes

1992 J. Phys.: Condens. Matter 4 5207

(http://iopscience.iop.org/0953-8984/4/22/018)

J. Phys.: Condens. Matter 4 (1992) 5207–5226. Printed in the UK

First-principles pseudopotential calculations for hydrogen in 4d transition metals: II. Vibrational states for interstitial hydrogen isotopes

C Elsässer†, K M Ho‡, C T Chan‡ and M Fähnle†

† Max-Planck-Institut für Metallforschung, Institut für Physik, Heisenbergstrasse 1, D-7000 Stuttgart 80, Federal Republic of Germany

‡ Ames Laboratory (USDOE) and Department of Physics, Iowa State University, Ames, Iowa 50011, USA

Received 23 December 1991

Abstract. In this second part of our first-principles study of hydrogen in transition metals within the framework of the Born–Oppenheimer and the local density-functional approximations, the mixed-basis pseudopotential method, which was outlined in the first part, is applied to calculate total energies and internal forces in Pd_nH supercells with $n \leqslant 32$ and Nb_nH supercells with $n \leqslant 4$. Adiabatic potentials for H in PdH and NbH are determined and the influence of lattice relaxations is discussed. Analytic model potentials are fitted to the first-principles results, and the importance of anharmonicity for vibrational states of interstitial H isotopes is investigated. By comparing our calculated vibrational energies with results from neutron-scattering experiments, we find that for NbH the anharmonicity is weak and the results obtained in harmonic approximation or via perturbation theory are in good agreement with experiment. For PdH the harmonic approximation as well as the perturbation theory are insufficient. The anharmonicity and the periodicity of the adiabatic potential need to be represented carefully by a Fourier series. Then the agreement with experiment is found to be as good as for NbH and even allows us to propose a reinterpretation of the experimental data.

1. Introduction

An important field of investigation in basic research as well as in technology is the study of hydrogen in metals and intermetallic compounds by virtue of the various interesting properties and technical implications (recent reviews were given by Völkl and Alefeld 1978a,b, Jena and Satterthwaite 1983, Schlapbach 1988). Depending on the host metal, it is possible to load the metal lattice with large amounts of hydrogen. The hydrogen atoms are distributed over interstitial lattice sites, and they often show a high mobility for diffusion. Both the high loading and mobility are important in technical applications, for example in the construction of hydrogen fuel storage for automobile engines.

From the viewpoint of basic research, the mechanism of hydrogen diffusion has been investigated extensively in both experiment and theory (see the review of Fukai and Sugimoto 1985). Microscopically diffusion can be related to local or collective vibrations of the light atoms around their interstitial sites (Flynn and Stoneham 1970, Kronmüller *et al* 1985). Another property related to these vibrations is the appearance

0953-8984/92/225207+20$04.50

of superconductivity in some metal hydrides like PdH (Skoskiewicz 1972), with a distinct inverse isotope effect of T_c (Stritzker and Buckel 1972).

Our present contribution consists of two parts. In the first part given previously (Ho *et al* 1991, denoted by I), we outlined our mixed-basis formalism for total energies and forces in transition-metal systems in the framework of the Born–Oppenheimer and local density-functional approximations (BOA and LDA).

In this second part we present a study at the microscopic level of vibrational states of hydrogen isotopes in transition metals by means of first-principles total-energy and force calculations (Elsässer 1990, Elsässer *et al* 1991a,b). We restrict ourselves to a discussion of the two systems PdH_x and NbH_x, (x is the hydrogen concentration), which are the most heavily investigated metal–hydrogen systems and therefore allow us to check the capability of our computational techniques by comparison with results from various experiments and other theories. Although there exists a rather large number of publications about first-principles electronic structure calculations for metal–hydrogen systems (see e.g. chapter 5 in Schlapbach 1988), total-energy and force calculations are as yet rare.

Hydrogen in body-centred cubic (BCC) niobium was studied by one of our groups some years ago (Ho *et al* 1984, Tao *et al* 1986). The results for electronic, cohesive, diffusion and vibrational properties for the two hydride phases β-NbH and γ-NbH were in good quantitative accordance with experiments. The success of this work motivated us to apply similar techniques to a study of hydrogen in face-centred cubic (FCC) palladium. Different hydrogen concentrations are investigated by using a series of cubic supercells Pd_nH ($n = 1/x = 1, 4, 8, 16, 32$), where the one interstitial H atom per unit cell is considered as a point defect in the host metal. We find that, especially for the vibrational properties, PdH turns out to be more complex than NbH and necessitates a more sophisticated treatment, which will be described in detail.

The paper is organized in the following way. In section 2 we give our results for the adiabatic potentials of hydrogen in γ-NbH and β-PdH. Calculated forces and influences of lattice relaxations in PdH_x are described in section 3. Section 4 contains our calculated results for vibrational states of hydrogen isotopes in the two cubic metals and a comparative discussion of our new results for β-PdH with the former results for γ-NbH (Tao *et al* 1986).

2. Adiabatic potentials for H in β-PdH and γ-NbH

Pure Pd and PdH_x ($0 < x < 1$) (see chapter 3 in Völkl and Alefeld 1978b) have FCC crystal lattices. The H atoms occupy stable interstitial sites within regular octahedra formed by six Pd atoms (see figure 1). PdH_x mainly exists in two phases: Low H concentrations ($x < 0.1$) yield the α phase in which the H atoms are distributed randomly over octahedral sites and are well separated from each other by several Pd atoms. At high H concentrations ($x > 0.6$), the Pd and H atoms form an almost stoichiometric compound PdH (β phase) with the rocksalt structure. For an investigation of both phases we performed calculations for several concentrations x by using different cubic supercells Pd_nH with periodic boundary conditions. The β phase is given by a Pd_1H unit cell. The isolated H atom in the Pd lattice of the α phase is approached by a series of supercells Pd_nH with $n = 1/x = 4, 8, 16, 32$.

For H in BCC Nb (see chapter 2 in Völkl and Alefeld 1978b), a series of cubic supercells was used correspondingly. The stable interstitial sites for H are in the

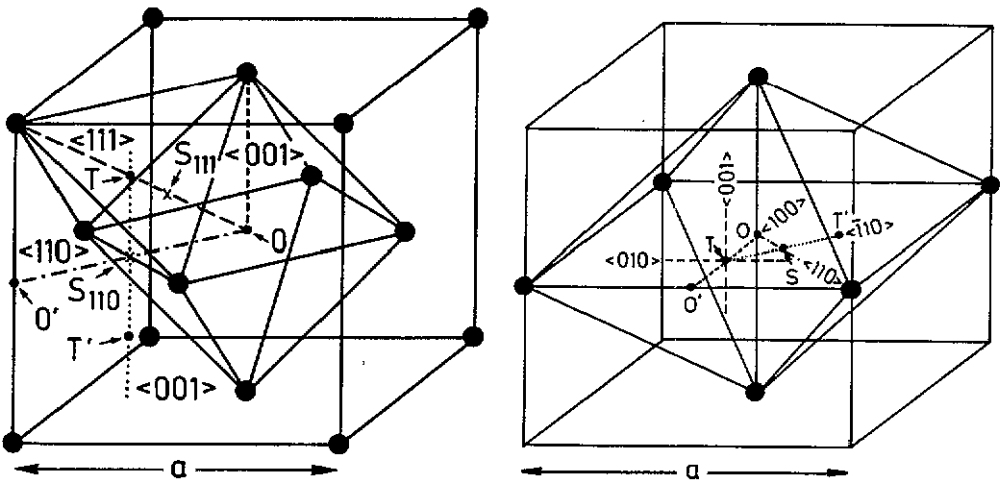

Figure 1. Interstitial sites and symmetry directions in a FCC Pd lattice (left) and in a BCC Nb lattice (right); O, O', octahedral sites; T, T', tetrahedral sites; S_{111}, S_{110}, S, saddle points; a = lattice constant.

middle of tetrahedra formed by four Nb atoms (see figure 1). At low concentrations, the H atoms are again randomly distributed over tetrahedral sites of the Nb lattice and form the α phase. For high concentrations an orthorhombic β phase is observed in experiments. It was shown by previous first-principles total-energy calculations (Tao *et al* 1986) that this phase is preferred also in theory over a pseudo-cubic γ phase. But whereas a hexagonal unit cell containing two Nb and two H atoms (Nb_2H_2) is required to describe the orthorhombic β phase, a BCC unit cell with each one Nb and one H atom (NbH) is sufficient for the γ phase. In this work we reproduce the results of Tao *et al* (1986) for the γ phase. In addition, the α phase is approached by cubic supercells Nb_nH ($n = 2, 4$) and lattice relaxations are studied for NbH.

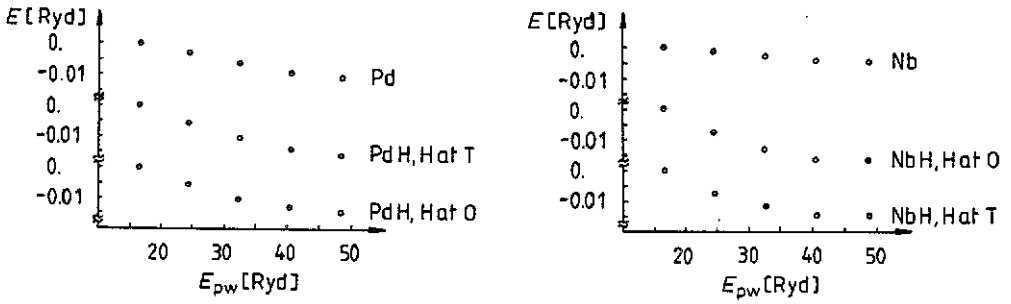

Figure 2. Convergence of total energies for Pd and PdH (left) and for Nb and NbH (right) with respect to the number of plane waves in the mixed basis; the total energies for E_{pw} = 16.5 Ryd are chosen as zero levels.

In the calculations for the metal–hydrogen systems, plane waves up to a maximum kinetic energy $|k + G|^2 = E_{pw}$ were included in the basis set. In addition five d-like localized functions per metal atom and one s-like function per H atom were included to represent effectively the localized character of the d and s states. To check the convergence of total-energy differences with respect to the completeness of the mixed

basis, total energies were calculated for Pd and PdH as well as for Nb and NbH for fixed lattice constants close to equilibrium as functions of E_{pw} (see figure 2). For the hydrides both octahedral and tetrahedral site occupations were considered. From E_{pw} = 16.5 Ryd to E_{pw} = 48.5 Ryd the changes in the energy differences for the two interstitial positions in the hydrides were less than 1 mRyd, whereas the absolute values of the total energies were shifted down by about 18 mRyd for PdH and 15 mRyd for NbH. Hence these shifts are almost independent of the H positions in the unit cell, and we assume that E_{pw} = 16.5 Ryd is sufficient for calculations of energy differences between the different H positions needed to map out the adiabatic potentials in the unit cells.

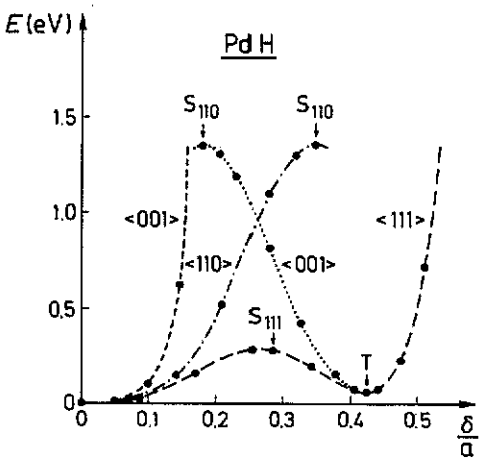

Figure 3. Energy–displacement curves for H in PdH (a = 4.07 Å): origin; octahedral minimum; T, tetrahedral minimum; S_{111}, S_{110}, saddle points.

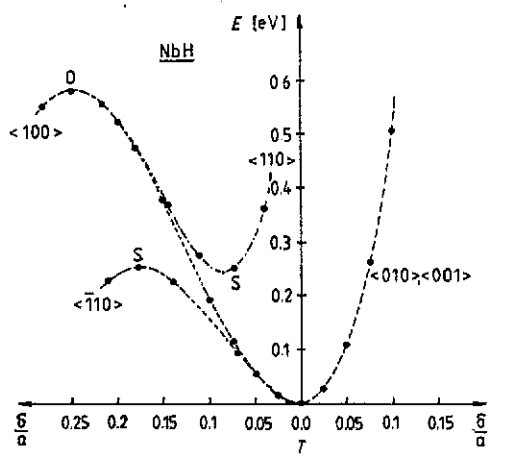

Figure 4. Energy–displacement curves for H in NbH (a = 3.41 Å): origin, tetrahedral minimum; O, octahedral saddle point; S, saddle point.

Table 1. Convergence of cohesive properties of PdH with respect to the number of k points in the IBZ; a_0 = equilibrium lattice constant; B_0 = bulk modulus; E_0 = cohesive energy.

H positions	k points	a_0 (Å)	B_0 (GPa)	E_0 (eV)
Oct. site	10	4.07	208	7.43
	60	4.07	209	7.42
Tet. site	10	4.18	175	7.34
	60	4.17	179	7.43

For the Brillouin-zone summations, simple-cubic grids of sampling points were used for all supercells. We found that meshes equivalent to 10 k points in the irreducible part of the first Brillouin zone (IBZ) of FCC Pd or eight k points in the IBZ of BCC Nb yielded sufficiently converged results for cohesive properties such as the equilibrium lattice constants a_0, the bulk moduli B_0 and the cohesive energies E_0 (see tables 1 and 2 for PdH and NbH, respectively). These quantities were found by calculating total energies for several lattice constants around equilibrium and fitting

a universal binding curve (Rose *et al* 1981) to these data points. This k-point grid was also used for the calculations of forces and relaxations in the supercells. For the calculation of the adiabatic potentials and vibration energies of PdH and NbH finer grids equivalent to 60 and 40 k points in the FCC and BCC IBZ, respectively, were used.

Table 2. Convergence of cohesive properties of NbH with respect to the number of k points in the IBZ: for a_0, B_0, E_0, see caption of table 1.

H positions	k points	a_0 (Å)	B_0 (GPa)	E_0 (eV)
Tet. site	12	3.42	206	12.47
	80	3.41	199	12.46
Oct. site	12	3.44	200	11.93
	80	3.44	186	11.89

The adiabatic potentials, i.e. the energy hyperfaces E_0^e, for H in PdH and NbH were determined by calculating total energies for H put at various positions while keeping the metal atom fixed at the origin in the unit cells. We shifted the H atom away from an octahedral site in PdH and from a tetrahedral site in NbH along several high-symmetry directions (see figure 1). The energy changes are displayed in figure 3 for PdH and figure 4 for NbH. The curves for PdH have already been discussed with respect to the diffusion of a classical particle (Elsässer *et al* 1991a). For NbH we essentially reproduced the results of Ho *et al* (1984). In figure 4 the curves along $\langle 110 \rangle$ and $\langle \bar{1}10 \rangle$ are added to point out the saddle point S at a lower energy than the octahedral site O, which itself turns out to be a saddle point in NbH.

3. Internal forces and lattice relaxations

In this section we give our results from the application of the mixed-basis force formalism described in I to Pd_nH supercells. Internal forces acting on the Pd atoms around a H atom in the supercells Pd_nH with $n = 1, 4, 8, 16, 32$ were calculated for cases where H was located at an octahedral site O, a tetrahedral site T, or a saddle point S_{111}, while the metal atoms were kept at the ideal lattice sites. The lattice constants of the supercells were fixed at the calculated equilibrium value $a_0 = 3.88$ Å of a pure Pd crystal ($a_{exp} = 3.89$ Å). The forces for the Pd_nH supercells with H at O or at T are compiled in table 3 or 4, respectively. The directions of the forces on the four Pd neighbour shells of H at O and T in $Pd_{32}H$ supercells are displayed in figure 5. In all supercells the directions of the forces fulfill all requirements of symmetry and translational periodicity, and we estimate a level of confidence of about ± 0.005 Ryd/au for the numerical values in tables 1–3.

Owing to the lattice symmetry the saddle point of the energy along the $\langle 111 \rangle$ direction is not exactly at the geometrical centre S_{111} of a Pd_3 triangle (see figure 1) but slightly shifted towards the octahedral site. Therefore a small force directed towards the tetrahedral site is acting on H at S_{111}. The geometric pattern of the forces for H at S_{111} is more complex than for H at the other two positions. But it is evident that the forces on the Pd atoms of the Pd_3 triangle next to H are directed to expand it. The forces for the different neighbour shells are given in table 5.

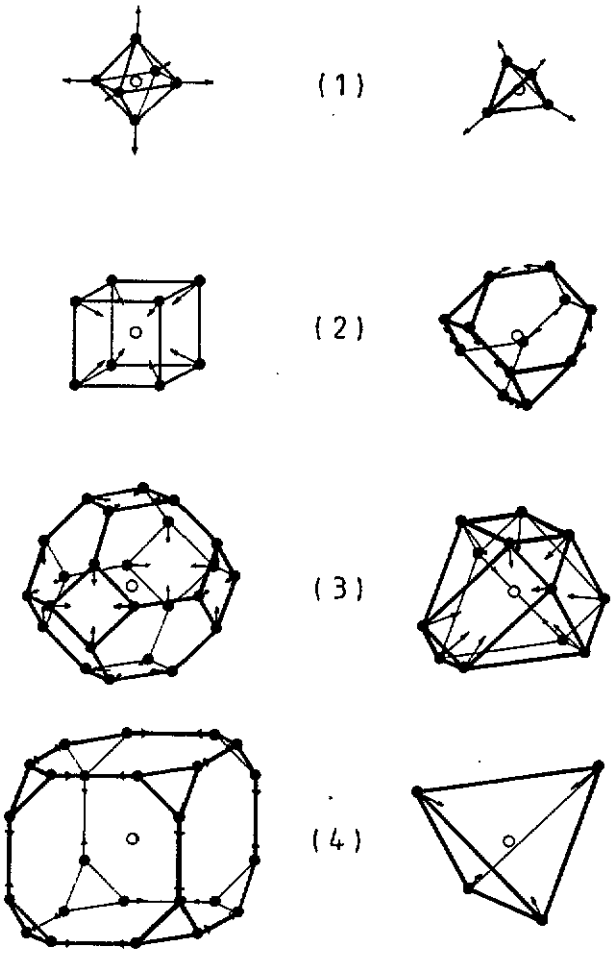

Figure 5. Directions of forces on the Pd atoms in $Pd_{32}H$ for H at an octahedral site (left) and at a tetrahedral site (right): o, H atom; •, Pd atoms; (1) – (4) denote the four different Pd shells (see tables 3 and 4).

Table 3. Magnitudes of forces F on the Pd atoms around an octahedral H atom in Pd_nH (Ryd/au): d/a = distance between Pd and H atom in units of the lattice constant $a = a_0(Pd) = 7.33$ au $= 3.88$ Å.

Shell	(1)	(2)	(3)	(4)
d/a	$\frac{1}{2}$	$\frac{1}{2}\sqrt{3}$	$\frac{1}{2}\sqrt{5}$	$\frac{3}{2}$
PdH	0.0	—	—	—
Pd_4H	0.0	0.0	—	—
Pd_8H	0.012	0.0	—	—
$Pd_{16}H$	0.012	0.0	0.0	—
$Pd_{32}H$	0.002	0.004	0.008	0.005

For H at the octahedral site, because of the high symmetry of the supercells, non-vanishing forces are only acting on the first-neighbour Pd atoms in the cells with $n < 16$. Forces on further shells appear in $Pd_{32}H$. All forces are rather small. This means that H on an octahedral site causes only a weak distortion of the Pd lattice.

For the two other H positions the forces on the first-neighbour Pd shells are

Table 4. Magnitudes of forces F on the Pd atoms around a tetrahedral H atom in Pd_nH (Ryd/au): see caption of table 3.

Shell d/a	(1) $\frac{1}{4}\sqrt{3}$	(2) $\frac{1}{4}\sqrt{11}$	(3) $\frac{1}{4}\sqrt{19}$	(4) $\frac{3}{4}\sqrt{3}$
PdH	0.0	—	—	—
Pd_4H	0.056	—	—	—
Pd_8H	0.063	0.001	—	—
$Pd_{16}H$	0.062	0.007	—	—
$Pd_{32}H$	0.060	0.003	0.008	0.006

Table 5. Magnitudes of forces F on the Pd atoms around a H atom located at a saddle point S_{111} in Pd_nH (Ryd/au): see caption of table 3.

Shell d/a	(1) $\frac{1}{6}\sqrt{6}$	(2) $\frac{1}{3}\sqrt{3}$	(3) $\frac{1}{2}\sqrt{2}$	(4) $\frac{1}{3}\sqrt{6}$	(5) $\frac{1}{6}\sqrt{30}$	(6) 1
PdH	0.0	—	—	—	—	—
Pd_4H	0.093	0.010	—	—	—	—
Pd_8H	0.103	0.011	0.003	—	—	—
$Pd_{16}H$	0.095	0.022	0.009	0.007	—	—
$Pd_{32}H$	0.096	0.012	0.002	0.004	0.004	0.009

Shell d/a	(7) $\frac{1}{6}\sqrt{42}$	(8) $\frac{2}{3}\sqrt{3}$	(9) $\frac{1}{2}\sqrt{6}$	(10) $\frac{1}{6}\sqrt{66}$	H 0
PdH	—	—	—	—	0.0
Pd_4H	—	—	—	—	0.002
Pd_8H	—	0.001	—	—	0.001
$Pd_{16}H$	—	—	0.005	—	0.000
$Pd_{32}H$	0.007	0.010	0.007	0.005	0.000

distinctly larger than those on the more distant shells. The force on the first shell is found to be almost independent of the supercell size. Hence the main reaction of the Pd lattice would be an expansion of the first shell. In fact, for the local lattice relaxations in Pd_4H and Pd_8H discussed below (see figure 6) it was sufficient to relax the first shell to get negligibly small forces for all shells.

From the essential independence of the forces on the first-neighbour Pd shell of the supercell size, we conclude that relatively small supercells can be useful for the modelling of isolated light interstitial particles like H in a transition metal. The dominant response of the metal lattice comes from the first-neighbour shell. However, the absolute values of the forces on the outer shells should not be taken too seriously because of the small size and the periodic boundary conditions of the supercells.

In the determination of adiabatic potentials in section 2 (see figures 3 and 4) the effects of lattice relaxations were not completely included. The volume of the unit cell was relaxed with H at the stable interstitial site and then kept fixed when the H was moved around. With the larger supercells Pd_nH and Nb_nH we can investigate the effects of relaxations via atomic displacements. The influence of such relaxations on the adiabatic potentials was already discussed earlier (Elsässer *et al* 1991a). But it would be a very laborious and time-consuming task to determine an adiabatic potential for Pd_nH or Nb_nH from first principles with the inclusion of relaxations of

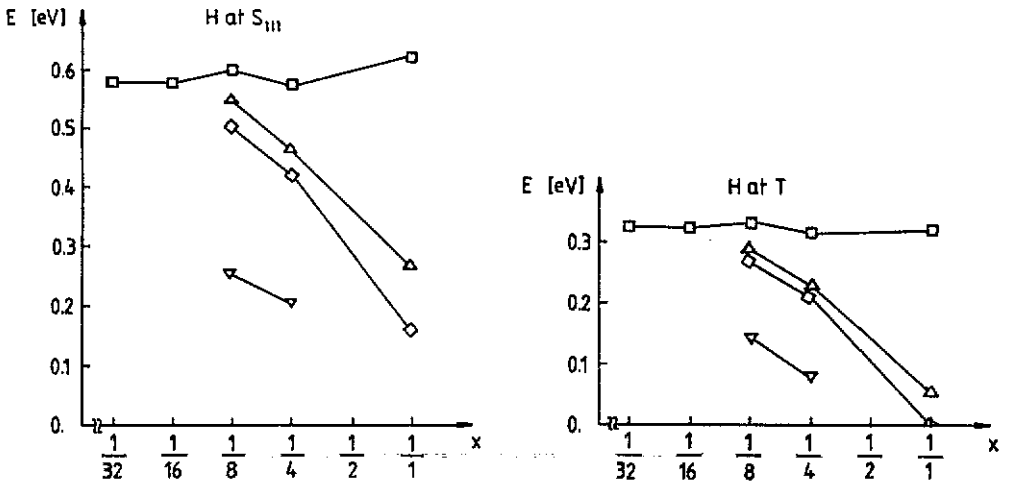

Figure 6. Energy differences for H at S_{111} (left) and at T (right) in PdH_x with respect to H at site O: □, $a = a_0(Pd) = 3.88$ Å; △, $a = a_0(PdH_x)$ with H at site O; ◇, a relaxed; ▽, a and Pd atoms relaxed.

both the volume and the atomic positions.

To study the effect of different stages of relaxations on the adiabatic potential in Pd_nH we restrict ourselves again to the energy differences for the special H positions at S_{111} or at T with respect to H at O (see figure 6). For H in the completely unrelaxed Pd lattice ($a = 3.88$ Å) the energy differences are large (□) and are almost independent of the H concentration. This indicates a relatively weak H–H interaction compared to the nearest-neighbour Pd–H interaction.

The first step of relaxation is an expansion of the unit-cell volume for H at O and keeping it fixed then for H at S_{111} or at T. These energy differences (▽) correspond to the situation in figure 3. The effect is very large for PdH but it decreases rapidly for lower concentrations. By further volume relaxation for H at S_{111} or at T the energy differences are lowered again but less drastically (◇). For PdH this is the fully relaxed state.

For lower H concentrations a further lowering of the energy differences can be achieved by local displacements of Pd atoms. This was done by shifting the Pd atoms until the calculated forces were negligibly small. As already mentioned above, shifts of only the Pd atoms next to the H atom turned out to be sufficient to reduce all forces below the limit of numerical significance. The energy differences for these final relaxed unit cells are denoted by △ in figure 6.

For Nb_nH ($n = 1, 2, 4$) a similar analysis of the energy differences for H at O or at S with respect to H at T (see figure 7) showed a much weaker influence of the volume relaxation for NbH than for PdH. Again, the energy differences for H in the unrelaxed Nb lattice ($a = 3.41$ Å, □) are essentially independent of the H concentration. But now the volume relaxation for H at T yields a lowering of the energy differences (△) by only a few per cents already for NbH. By further volume relaxations for H at O or S the lowerings of the energy differences were negligible. This leads us to the assumption that lattice relaxations have a much less important influence on the adiabatic potential for H in Nb than in Pd, probably because of the more open packing of the BCC crystal lattice.

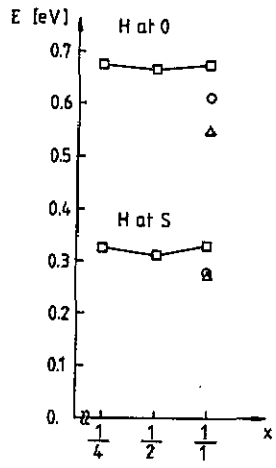

Figure 7. Energy differences for H at S and at O in NbH_x with respect to H at site T: □, $a = a_0(Nb) = 3.23$ Å; △, $a = a_0(NbH_x)$ with H at site T; ○, results from Tao *et al* (1986) for γ-NbH.

To test the possibility of a stabilization of the octahedral saddle point by local relaxations in a BCC lattice, which is discussed for low H concentrations (Puska and Nieminen 1984, Fritzsche *et al* 1990), many total-energy calculations for large supercells or an alternative approach via a Green function method would be required.

In our first-principles calculations the atomic nuclei are considered to be point-like, i.e. having infinite mass compared to the electrons. For light particles like H isotopes, the spatial extension of the nuclear wavefunctions has to be considered, e.g. for the study of isotope effects in the diffusion or self-trapping of the particles. In future studies, we intend to approach such problems by linking our *ab initio* method with an empirical scheme of Klamt and Teichler (1986, see also Sugimoto and Fukai 1982, Puska and Nieminen 1984, Christodoulos and Gillan 1991) with a fit of the empirical parameters to *ab initio* data.

4. Vibrational states for H in β-PdH and γ-NbH

Vibrational properties of interstitial H in Nb (Richter and Shapiro 1980, Rush *et al* 1981, Eckert *et al* 1983) and Pd (Drexel *et al* 1976, Rush *et al* 1984) single crystals were studied experimentally via inelastic neutron scattering (INS; see chapter 4 in Völkl and Alefeld 1978b). Line intensities and shapes of the measured excitation spectra were commonly interpreted in terms of oscillator states of the light particle in a three-dimensional potential well, either in the harmonic approximation (Schober and Lottner 1979) or by taking anharmonicity into account via perturbation theory (Eckert *et al* 1983, Rush *et al* 1984). Theoretically, energies and wavefunctions of H vibrational states in BCC and FCC metals were calculated using empirical (Sugimoto and Fukai 1982, Klamt and Teichler 1986, Christodoulos and Gillan 1991) or parameter-free (Puska and Nieminen 1984) model theories. Although anharmonicity can be taken into account beyond perturbation theory in such studies, rather crude approximations are necessary for the interaction potentials, and the parametrization of the empirical models strongly depends on accurate experimental data which are usually available only for a limited number of systems.

Some years ago the vibrational potential and excitation energies for H in the γ phase NbH were calculated from first principles (Ho *et al* 1984, Tao *et al* 1986), and the results were in quantitative agreement with the available INS data. The success of this work motivated us to apply similar techniques to the case of H in PdH and Pd_4H (Elsässer *et al* 1991b), which revealed a more complicated behaviour.

In this section we give a comparison of our results for PdH and NbH with emphasis on the importance of anharmonicity. It will be demonstrated that for H on tetrahedral sites in Nb the harmonic approximation suffices, whereas for H on octahedral sites in Pd there is a strong anharmonicity and anisotropy of the potential, and a harmonic or perturbative calculation of vibrational states is quantitatively inadequate.

For the vibrational states in the metal hydrides we assumed the BOA once again for the heavy metal atoms and the light hydrogen isotopes. Hydrogen was considered to vibrate in a stiff metal lattice. The vibrational states were determined by solving the Schrödinger equation of a particle moving in a three-dimensional potential. The potential in the BOA was represented by fits of analytical functions $V(x,y,z)$ to the first-principles data (x,y,z are Cartesian coordinates). We applied two different kinds of function $V(x,y,z)$.

In one approach we followed the suggestions given in the literature (Eckert *et al* 1983, Rush *et al* 1984) for the interpretation of INS spectra via polynomial potential wells that are centred at the local potential minima and have the correct point symmetries. Up to fourth order in the Cartesian coordinates, for an octahedral or a tetrahedral site in FCC Pd the potential $V(x,y,z)$ is given by (see appendix 2)

$$V(x,y,z) = c_2(x^2+y^2+z^2) + c_3xyz + c_4(x^4+y^4+z^4) + c_{22}(x^2y^2+y^2z^2+z^2x^2) \tag{1}$$

with $c_3 = 0$ for the octahedral site, and for a tetrahedral site in BCC NbH (see appendix 3) by

$$V(x,y,z) = c_{2,x}(x^2+y^2) + c_{2,z}z^2 + e(x^2-y^2)z + c_{4,x}(x^4+y^4) + c_{4,z}z^4 + fx^2y^2 + g(x^2+y^2)z^2. \tag{2}$$

The coefficients were determined by least-squares fits to nine, seven and 12 first-principles data points surrounding a Pd octahedral, tetrahedral and Nb tetrahedral site, respectively (see figures 3 and 4). Corrections to the eigenstates of a three-dimensional harmonic oscillator (second-order potential terms) due to the anharmonicity of the potentials are calculated using standard perturbation theory (see appendices 1–3). The fourth-order potential terms lead to first-order perturbation corrections, and the third-order terms to second-order corrections.

In an alternative approach a finite, three-dimensional Fourier series was fitted to all available energy versus displacement data throughout the whole unit cells (see figures 3 and 4):

$$V(r) = \sum_G V(G)\exp(iG\cdot r). \tag{3}$$

In contrast to the local potential wells given above, this function takes both the translational periodicity of the potential and the saddle points between the different local

minima into account. For PdH we fitted the Fourier components of 19 independent stars of reciprocal lattice vectors G to the energies of all 30 different H positions shown in figure 3. Then the three-dimensional Schrödinger equation for H isotopes in the periodic potential was expanded in plane waves and diagonalized numerically for the Γ point ($k = 0$):

$$\sum_{G'} \left(\frac{|G|^2}{m_H} \delta_{G,G'} + V(G - G') \right) \phi_{|\mu\rangle}(G') = E_{|\mu\rangle} \phi_{|\mu\rangle}(G). \tag{4}$$

In this approach for PdH, which corresponds to the one described by Tao *et al* (1986) for NbH, anharmonicity is treated completely, not as a perturbation. The low-lying eigenstates $\phi_{|\mu\rangle}$ can be associated with the corresponding states $|\mu\rangle$ found for the local potential wells discussed above.

Our calculated zero-point and excitation energies, $E_{0,|000\rangle}$ and $e_{M,|\mu\rangle} = E_{M,|\mu\rangle} - E_{0,|000\rangle}$, for three H isotopes are compiled and compared with experimental data in the tables 6–8. For the ground and the low excited states it is possible to classify the states obtained numerically or via perturbation theory by the corresponding states in harmonic approximation. The index $M = n + m + l$ gives the number of energy quanta, and $|mu\rangle$ indicates the eigenfunction of the excited state (see appendices 2 and 3). For NbH we did not repeat the expensive calculation with the Fourier potential. Instead we relist the results from Tao *et al* (1986) for comparison in our table 6.

The data of table 6 show that for H in Nb the measured vibration energies are described already quite well by the local polynomial potential in harmonic approximation (a). Taking the anharmonicity (b) or both anharmonicity and periodicity ((c), from Tao *et al* 1986) of the potential into account does not improve the agreement of the calculation and experiment significantly. It is concluded that the considered lowest vibration states are confined to a tetrahedral site in the BCC Nb. The anharmonicity is weak and can be treated well via perturbation theory.

For vibrations of H around the octahedral site in Pd the energies calculated with the polynomial potential do not agree with measured INS data, as shown in table 7. The harmonic approximation (a) yields energies that are significantly too low. By taking the anharmonicity into account via perturbation theory (b) the energies become muc. too high. The origin for these discrepancies is the strong anisotropy and anharmonicity of the adiabatic potential, which is described poorly by a local polynomial function. The perturbative approach is also questionable in the presence of strong anharmonicity. In contrast, the vibrational energies calculated with the Fourier potential (c), which is not confined to the local surrounding of an octahedral site, agree much better with the available INS data. The conclusion is that the anharmonicity of the potential needs to be taken into account completely already for the lowest states.

Some remarks are necessary concerning the comparison of calculated and measured energies. First, in the INS experiments (Rush *et al* 1984) the higher excitation energies in Pd were measured in α-phase samples with low H concentrations, whereas the PdH unit cell used in our calculations corresponds to the β phase with high H concentration. In our calculations with Pd_nH supercells (n = 4, 8, 16, 32) to approach the α phase (Elsässer *et al* 1991a) we found that the decreasing H concentration leads to a reduction of the equilibrium lattice constant of the ideal FCC lattice. This is connected with a steeper vibrational potential and higher vibration

Table 6. Zero-point energies $E_{0,|000\rangle}$ and excitation energies $e_{M,|\mu\rangle}$ of local tetrahedral vibrations of hydrogen isotopes in NbH ($a = 3.41$ Å): (*a*) harmonic approximation; (*b*) perturbation theory; (*c*) solution of Fourier representation. The meaning of $|Q\rangle$ is specified in appendix 3. The experimental data are taken from Richter and Shapiro (1980), Rush *et al* (1981) and Eckert *et al* (1983), the calculated data (*c*) for γ-NbH from Tao *et al* (1986).

		^{1}H	^{2}D	^{3}T
$E_{0,\|000\rangle}$	(a)	239	169	138
	(b)	243	171	139
	(c)	237	169	139
$e_{1,\|001\rangle}$	(a)	126	89	73
	(b)	114	83	69
	(c)	113	84	70
Expt.		122 ± 1	86.7 ± 0.9	72 ± 1
$e_{1,\|010\rangle} = e_{1,\|100\rangle}$	(a)	176	124	101
	(b)	165	119	98
	(c)	161	118	98
Expt.		166 ± 2	120.7 ± 0.9	101 ± 1
$e_{2,\|Q\rangle}$	(a)	253	178	146
	(b)	223	164	136
	(c)	218	161	136
Expt.		231 ± 2	166 ± 3	
$e_{2,\|101\rangle} = e_{2,\|011\rangle}$	(a)	302	214	174
	(b)	268	196	163
	(c)	257	195	164
Expt.		280 ± 4	205 ± 5	

energies. By taking lattice relaxations into account we found that local volumes of the Pd octahedra around the interstitial H in Pd_4H and Pd_8H were slightly smaller than for H as in PdH. This is consistent with the experimental observation of Rush *et al* (1984), where for the first excited states of H the measured energies are 69 meV for the α phase and 60 meV for the β phase (see figure 2 in Rush *et al* 1984).

Secondly, in the interpretation of their INS spectra, besides the large peak from the first excitation, e_{100}, Rush *et al* (1984) identified two further structures as three-fold degenerate excitations e_{110} and e_{200} (see figure 1 in Rush *et al* 1984). In a cubic environment, the six degenerate harmonic states with $M = 2$ split into three levels: a triply degenerate, $E_{2,|011\rangle} = E_{2,|101\rangle} = E_{2,|110\rangle}$, a doubly degenerate, $E_{2,|A\rangle} = E_{2,|B\rangle}$, and a single level, $E_{2,|C\rangle}$ (see appendix 2). Comparing our calculated vibration energies with the INS spectra of Rush *et al* (1984) we propose the following interpretation (see table 7). The two structures at 137 ± 2 meV and 156 ± 3 meV seem to be the excitations $e_{2,|C\rangle}$ and $e_{2,|A\rangle} = e_{2,|B\rangle}$, respectively. The remaining excitations $e_{2,|011\rangle} = e_{2,|101\rangle} = e_{2,|110\rangle}$ might be located around 115 ± 5 meV where the noise in the spectra does not obviously exclude a third small structure.

Thirdly, for the lowest vibrational energies of tritium in Pd, one should be aware of the fact that the energy range of phonons of the Pd lattice is measured from 0 to about 23 meV in $PdH_{0.63}$ (Rowe *et al* 1974) and to about 29 meV in pure

Table 7. Zero-point energies $E_{0,|000\rangle}$ and excitation energies $e_{M,|\mu\rangle}$ of local octahedral vibrations of hydrogen isotopes in PdH ($a = 4.07$ Å): for (a), (b), (c); see caption of table 6. The meaning of $|A\rangle$, $|B\rangle$ and $|C\rangle$ is specified in appendix 3. The experimental data are taken from Rush *et al* (1984); α and β denote the phases.

		^{1}H	^{2}D	^{3}T
$E_{0,\|000\rangle}$	(a)	50	36	29
	(b)	120	70	52
	(c)	78	51	40
$e_{1,\|100\rangle} = e_{1,\|010\rangle} = e_{1,\|001\rangle}$	(a)	34	23	20
	(b)	126	70	50
	(c)	62	40	32
Expt.	β	60	40	
	α	69.0 ± 0.5	46.5 ± 0.5	
$e_{2,\|011\rangle} = e_{2,\|101\rangle} = e_{2,\|110\rangle}$	(a)	68	47	39
	(b)	226	127	92
	(c)	117	78	61
Expt.	α	115 ± 5		
$e_{2,\|C\rangle}$	(a)	68	47	39
	(b)	344	186	131
	(c)	132	88	69
Expt.	α	137 ± 2		
$e_{2,\|A\rangle} = e_{2,\|B\rangle}$	(a)	68	47	39
	(b)	383	206	144
	(c)	147	94	73
Expt.	α	156 ± 3		

Table 8. Zero-point energies $E_{0,|000\rangle}$ and excitation energies $e_{M,|\mu\rangle}$ of local tetrahedral vibrations of hydrogen isotopes in PdH ($a = 4.07$ Å): for (a), (b), (c), see caption of table 6.

		^{1}H	^{2}D	^{3}T
$E^{tet}_{0,\|000\rangle}$	(a)	204	144	117
	(b)	208	146	119
	(c)	213	150	123
$e^{tet}_{1,\|100\rangle} = e^{tet}_{1,\|010\rangle} = e^{tet}_{1,\|001\rangle}$	(a)	136	96	78
	(b)	124	90	75
	(c)		92	77

Pd (Miller and Brockhouse 1971). It has been suggested that the localization of the tritium vibrations, whose zero-point energies are close to these ranges, can be destroyed by resonance with the metal phonons and thus might be not observable directly (Oppeneer *et al* 1988).

Besides the H vibrations around stable octahedral sites in PdH, we also investigated the possibility for metastable H states confined to tetrahedral sites. With the polynomial potential, zero-point and first excitation energies were calculated in the harmonic approximation and with perturbation theory. They show that the local po-

tential around a tetrahedral site is only weakly anharmonic. In table 8 they are listed, together with energies found with the Fourier potential, which can be associated to tetrahedral sites via symmetry and convergence arguments. The energies are referred to the tetrahedral minimum, which is 51 meV above the octahedral minimum (see figure 3). Metastable bound states at tetrahedral sites can be expected at least if the zero-point energies are below the depth of the local potential well, which is limited by the difference of 215 meV between the minimum at T and the saddle-point energy at S_{111}. This implies that an occupation of a tetrahedral site is more likely for ^{3}T or ^{2}D than for ^{1}H.

The occupations of interstitial sites in FCC Pd were investigated by means of ion channeling experiments (Carstanjen 1989). For PdH_x and PdD_x at and above room temperatures, where the thermal vibration amplitudes of the interstitials around octahedral sites are already rather large, no evidence was found for occupations of tetrahedral sites. According to our calculations we would expect to find a channelling signal along crystalline ⟨100⟩ directions originating from a few interstitials trapped in metastable tetrahedral sites for the isotope ^{3}T and eventually ^{2}D at low temperatures, where the ⟨100⟩ blocking originating from octahedral-site occupation is less smeared out by the thermal vibrations. An occupation of tetrahedral sites by ^{3}T would also be compatible with the observed anomalous isotope effect for activation energies of H diffusion in Pd (Teichler 1979, Kronmüller *et al* 1985).

5. Summary

In this paper, which is the second of two papers about our first-principles study of hydrogen in transition metals, we reported the results of total-energy and force calculations for Pd_nH supercells with $n \leqslant 32$ and for Nb_nH supercells with $n \leqslant 4$, using a mixed-basis pseudopotential method, which was outlined in part I.

Our project was concerned with the development of a calculational method for excitation energies of local vibrations of interstitial hydrogen isotopes in transition metals. To test the capability of our approach we chose FCC Pd and BCC Nb for our study, the two most heavily investigated metal hosts for hydrogen, with a large pool of existing experimental and theoretical information for comparison.

Within the framework of the BOA and the LDA, adiabatic potentials for H in PdH and NbH were determined. The influence of different stages of lattice relaxations on the adiabatic potentials in the supercells was discussed. From both total-energy differences and internal forces in the supercells we deduced that the dominant contribution to lattice relaxations around an interstitial H atom in Pd comes from a local expansion on the next-neighbour Pd atoms. For H in BCC Nb we found a much weaker influence of lattice relaxations on the adiabatic potential than in FCC Pd.

By fitting analytic model potentials to the adiabatic potentials determined from first principles we calculated vibrational states for hydrogen isotopes in γ-NbH and in β-PdH and studied the influence of anharmonicity.

For NbH we found that excitation energies for several vibrational states, which were calculated using a simple local potential well in harmonic approximation or by taking anharmonicity into account as a perturbation, agreed very well both with earlier calculations using a Fourier fit of the adiabatic potential and a non-perturbative treatment of the vibrational states and with measured data from INS experiments.

For PdH a simple local potential well and the calculation of vibrational states in harmonic approximation or via perturbation theory turned out to be quantitatively

inadequate. Because of the strong anharmonicity and the rather low vibrational energies, the adiabatic potential had to be represented carefully by a Fourier series. The excitation energies finally found by solving the proton Schrödinger equation in a plane-wave representation were in good agreement with experimental data and even allowed us to propose a reinterpretation of measured INS spectra.

The success of our calculations for PdH and NbH encourages us to proceed in two directions. First, we expect to find reliable vibrational energies as well for other metals or intermetallic compounds. These may be of use for the interpretation of diffusion experiments, where no INS data are yet available or are difficult to measure, e.g. for hydrogen in Fe because of the low solubility, or for tritium in any metal because of its toxicity. Second the *ab initio* results seem to be reliable enough to be useful for the calibration of more empirical theories.

Acknowledgments

The Ames Laboratory is operated for the US Department of Energy by the Iowa State University under Contract No. W-7405-Eng-82. The work was supported in part by the Director for Energy Research, Office of Basic Energy Sciences, including a grant of computer time on the Cray computers at the NERSC in Livermore, California.

Appendix 1. Perturbation theory for degenerate states

In this appendix we briefly summarize the formalism of time-independent perturbation theory for partly degenerate vibrational states. One reason is that, although perturbation theory is well known from almost every lecture or textbook about quantum mechanics (see e.g. Blochinzew 1985), its application to vibrational states is rapidly becoming laborious. Therefore we want to provide our derived expressions to the readership for further use.

The other and main reason, however, for this appendix is that the splitting of degenerate harmonic states in cubic lattices, which require the rigorous application of degenerate perturbation theory, is not fully included in earlier publications (Eckert *et al* 1983, Rush *et al* 1984, Kronmüller et al. 1985, Oppeneer *et al* 1988). Some authors give general formulae for arbitrary states which, however, do not take all splittings into account. There are also discrepancies between the formulae in different papers. These ambiguities and inconsistencies caused us to rederive carefully the expressions for energy corrections of some states, taking the degeneracies into account. Further states can be treated in the same way. But we could not find general formulae for arbitrary states in cubic lattices that yield all splittings correctly.

The basic equation for degenerate perturbation theory is the *secular equation*:

$$\sum_{\nu}\langle\phi^{(0)}_{m\mu}|V_a|\phi^{(0)}_{m\nu}\rangle c^m_{\kappa\nu} = E^{(1)}_{m\kappa}c^m_{\kappa\mu} \tag{A1.1}$$

where the potential V_a is the anharmonic part of the vibration potential $V = V_h + V_a$. The $|\phi^{(0)}_{m\mu}\rangle$ are the eigenstates of the harmonic part V_h (zeroth order), with the eigenvalues $E^{(0)}_{m\mu} = E^{(0)}_m$. The index m labels different harmonic levels, $\mu = 1, \ldots,$ and f_m the different degenerate states of one level.

The first-order energy corrections $E^{(1)}_{m\mu}$ are given by the solution of the *secular determinant*:

$$\det\left|\langle\phi^{(0)}_{m\mu}|V_a|\phi^{(0)}_{m\nu}\rangle - E^{(1)}_{m\mu}\delta_{\mu\nu}\right| = 0 \tag{A1.2}$$

and the components $c^m_{\kappa\nu}$ of the eigenvectors of (A1.1) rotate the zeroth-order basis set $\left\{|\phi^{(0)}_{m\mu}\rangle\right\}$ in the degenerate mth subspace to a new set $\left\{|\psi^{(0)}_{m\kappa}\rangle\right\}$ where

$$|\psi^{(0)}_{m\kappa}\rangle = \sum_{\nu=1}^{f_m} c^m_{\kappa\nu}|\phi^{(0)}_{m\nu}\rangle \tag{A1.3}$$

for which the perturbation matrix becomes diagonal,

$$\langle\psi^{(0)}_{m\mu}|V_a|\psi^{(0)}_{m\nu}\rangle = E^{(1)}_{m\mu}\delta_{\mu\nu} \tag{A1.4}$$

with the first-order energy corrections $E^{(1)}_{m\mu}$ as diagonal elements.

The second-order energy corrections $E^{(2)}_{m\mu}$ of the mth state are obtained by summing over all other states $k\kappa$ ($k \neq m$):

$$E^{(2)}_{m\mu} = \sum_{k(\neq m)}\sum_{\kappa=1}^{f_k}\frac{\left|\langle\psi^{(0)}_{m\mu}|V_a|\psi^{(0)}_{k\kappa}\rangle\right|^2}{E^{(0)}_m - E^{(0)}_k} = \sum_{k(\neq m)}\sum_{\kappa=1}^{f_k}\frac{\left|\langle\psi^{(0)}_{m\mu}|V_a|\phi^{(0)}_{k\kappa}\rangle\right|^2}{E^{(0)}_m - E^{(0)}_k}. \tag{A1.5}$$

In the last equation the orthogonality and completeness of the basis sets are used, which follow from the hermiticity of the perturbation matrix $\langle\phi^{(0)}_{m\mu}|V_a|\phi^{(0)}_{m\nu}\rangle$:

$$\sum_\nu c^m_{\kappa\nu}c^m_{\kappa'\nu} = \delta_{\kappa,\kappa'} \qquad \sum_\kappa c^m_{\kappa\nu}c^m_{\kappa\nu'} = \delta_{\nu,\nu'}. \tag{A1.6}$$

Appendix 2. Local vibrations of interstitials in a FCC crystal

The three-dimensional vibrational potential for a light interstitial particle in a FCC lattice can be described by a polynomial expansion up to fourth order in Cartesian coordinates (Rush *et al* 1984):

$$V(x,y,z) = V_h(x,y,z) + V_a(x,y,z) \tag{A2.1}$$

with the harmonic part

$$V_h(x,y,z) = c_2(x^2+y^2+z^2) \tag{A2.2}$$

and the lowest anharmonic terms:

$$V_a(x,y,z) = c_3xyz + c_4(x^4+y^4+z^4) + c_{22}(x^2y^2+y^2z^2+z^2x^2). \tag{A2.3}$$

The eigenvalues of the harmonic oscillator $V_h(x,y,z)$ are given by

$$E_{|nml\rangle} = \alpha\left(\tfrac{3}{2}+n+m+l\right) \qquad n,m,l = 0,1,2,\ldots \tag{A2.4}$$

with the energy quantum

$$\alpha = \hbar\omega_0 = \hbar\sqrt{(2c_2/m_H)}^{1/2}$$

and the mass m_H of a hydrogen isotope. The eigenstates $|nml\rangle$ of the energy level $M = n+m+l$ are $\frac{1}{2}(M+1)(M+2)$-fold degenerate. In the following we restrict ourselves to the states with $M = 0, 1, 2$.

Applying the formalism of degenerate perturbation theory to the anharmonic potential $V_a(x, y, z)$ it turns out that the third-order potential term does not contribute to the first-order energy corrections $E^{(1)}_{M\mu}$, and for the second-order corrections $E^{(2)}_{M\mu}$ the sum in (A1.5) can be separated into two sums containing the matrix elements of only third- or fourth-order potential terms, respectively. The first-order energy corrections are proportional to the potential parameters c_3, c_4 and c_{22}, the second-order corrections to their squares. The potential parameter c_3 is zero for the octahedral interstitial site. But for the tetrahedral site in Pd c_3 is about one order of magnitude larger than c_4 and c_{22}. This justifies the approximation to neglect the second-order corrections originating from c_4 and c_{22}. Hence the following energies $E_{M,|\mu\rangle}$ for the states with $M = 0, 1, 2$ contain the harmonic energies, the first-order corrections due to the fourth-order potential terms and the second-order corrections due to the third-order potential terms:

$$E_{M,|\mu\rangle} = E^{(0)}_{nml} + E^{(1)}_{M,|\mu\rangle} + E^{(2)}_{M,|\mu\rangle}$$

$$E_{0,|000\rangle} = \tfrac{3}{2}\alpha + \tfrac{3}{2}\beta + \tfrac{3}{2}\gamma - \tfrac{1}{2}\delta$$

$$E_{1,|100\rangle} = E_{1,|010\rangle} = E_{1,|001\rangle} = \tfrac{5}{2}\alpha + \tfrac{7}{2}\beta + \tfrac{7}{2}\gamma - \tfrac{5}{2}\delta$$

$$E_{2,|011\rangle} = E_{2,|101\rangle} = E_{2,|110\rangle} = \tfrac{7}{2}\alpha + \tfrac{11}{2}\beta + \tfrac{15}{2}\gamma - \tfrac{1}{2}\delta$$

$$E_{2,|A\rangle} = E_{2,|B\rangle} = \tfrac{7}{2}\alpha + \tfrac{15}{2}\beta + \tfrac{9}{2}\gamma - \tfrac{3}{2}\delta$$

$$E_{2,|C\rangle} = \tfrac{7}{2}\alpha + \tfrac{15}{2}\beta + \tfrac{15}{2}\gamma - \tfrac{21}{2}\delta$$

with the anharmonic coefficients

$$\beta = \tfrac{3}{2}x_0^4 c_4 \qquad \gamma = \tfrac{1}{2}x_0^4 c_{22} \qquad \delta = x_0^6 c_3^2/(12\hbar\omega_0)$$

and $x_0^2 = \hbar/m_H\omega_0$. Here $|A\rangle$, $|B\rangle$ and $|C\rangle$ are rotated basis states which diagonalize the perturbation matrix:

$$|A\rangle = (1/\sqrt{2})(|200\rangle - |020\rangle)$$

$$|B\rangle = (1/\sqrt{6})(|200\rangle + |020\rangle - 2|002\rangle)$$

$$|C\rangle = (1/\sqrt{3})(|200\rangle + |020\rangle + |002\rangle).$$

Appendix 3. Local vibrations of interstitials in a BCC crystal

For the vibrations of a light particle around a tetrahedral site in a BCC lattice the potential is approximated by (Eckert *et al* 1983):

$$V(x,y,z) = V_h(x,y,z) + V_a(x,y,z) \tag{A3.1}$$

with

$$V_h(x,y,z) = c_{2,x}(x^2+y^2) + c_{2,z}z^2 \tag{A3.2}$$

and

$$V_a(x,y,z) = e(x^2-y^2)z + c_{4,x}(x^4+y^4) + c_{4,z}z^4 + fx^2y^2 + g(x^2+y^2)z^2. \tag{A3.3}$$

For the harmonic oscillator $V_h(x,y,z)$ the energy eigenvalues are given by

$$E^{(0)}_{|nml\rangle} = \hbar\omega_x(1+n+m) + \hbar\omega_z(\tfrac{1}{2}+l) \qquad n,m,l = 0,1,2,\ldots \tag{A3.4}$$

with the energy quanta

$$\hbar\omega_x = \hbar(2c_{2,x}/m_H)^{1/2} \qquad \hbar\omega_z = \hbar(2c_{2,z}/m_H)^{1/2}$$

and the partly degenerate eigenstates $|nml\rangle$.

As in the case of the FCC lattice only fourth-order potential terms yield first-order corrections to the energies, and second-order corrections can be separated in each a contribution from third- and fourth-order potential terms. The fourth-order contribution is again negligibly small compared to the third-order contribution for the tetrahedral site in niobium. The resulting energies of the vibration states $|\mu\rangle$ are

$$E_{M,|\mu\rangle} = E^{(0)}_{|nml\rangle} + E^{(1)}_{M,|\mu\rangle} + E^{(2)}_{M,|\mu\rangle}. \tag{A3.5}$$

The first-order corrections are

$$E^{(1)}_{0,|000\rangle} = 6c_{4,x}\epsilon_x^2 + 3c_{4,z}\epsilon_z^2 + f\epsilon_x^2 + 2g\epsilon_x\epsilon_z$$

$$E^{(1)}_{1,|100\rangle} = E^{(1)}_{1,|010\rangle} = 18c_{4,x}\epsilon_x^2 + 3c_{4,z}\epsilon_z^2 + 3f\epsilon_x^2 + 4g\epsilon_x\epsilon_z$$

$$E^{(1)}_{1,|001\rangle} = 6c_{4,x}\epsilon_x^2 + 15c_{4,z}\epsilon_z^2 + 3f\epsilon_x^2 + 12g\epsilon_x\epsilon_z$$

$$E^{(1)}_{2,|011\rangle} = E^{(1)}_{2,|101\rangle} = 18c_{4,x}\epsilon_x^2 + 15c_{4,z}\epsilon_z^2 + 3f\epsilon_x^2 + 12g\epsilon_x\epsilon_z$$

$$E^{(1)}_{2,|110\rangle} = 30c_{4,x}\epsilon_x^2 + 3c_{4,z}\epsilon_z^2 + 9f\epsilon_x^2 + 6g\epsilon_x\epsilon_z$$

with

$$\epsilon_x = \tfrac{1}{2}x_0^2 = \hbar/(2m_H\omega_x) \qquad \epsilon_z = \tfrac{1}{2}z_0^2 = \hbar/(2m_H\omega_z)$$

and

$$E^{(1)}_{2,|A\rangle} = a - c$$
$$E^{(1)}_{2,|P\rangle} = \tfrac{1}{2}\{a + b + c + [(a + b + c)^2 + 8d^2]^{1/2}\}$$
$$E^{(1)}_{2,|Q\rangle} = \tfrac{1}{2}\{a + b + c - [(a + b + c)^2 + 8d^2]^{1/2}\}$$

with

$$a = 42c_{4,x}\epsilon_x^2 + 3c_{4,z}\epsilon_z^2 + 5f\epsilon_x^2 + 6g\epsilon_x\epsilon_z$$
$$b = 6c_{4,x}\epsilon_x^2 + 39c_{4,z}\epsilon_z^2 + f\epsilon_x^2 + 10g\epsilon_x\epsilon_z$$
$$c = 2f\epsilon_x^2$$
$$d = 2g\epsilon_x\epsilon_z.$$

The rotated basis states $|A\rangle$, $|P\rangle$, $|Q\rangle$ are given by the linear combinations

$$|A\rangle = (1/\sqrt{2})(|200\rangle - |020\rangle)$$
$$|P\rangle = [1/(2p^2 + 1)^{1/2}](p|200\rangle + p|020\rangle + |002\rangle)$$
$$|Q\rangle = [1/(2q^2 + 1)^{1/2}](q|200\rangle + q|020\rangle + |002\rangle)$$

with

$$p = (1/4d)\{a - b + c + [(a - b + c)^2 + 8d^2]^{1/2}\}$$
$$q = (1/4d)\{a - b + c - [(a - b + c)^2 + 8d^2]^{1/2}\}.$$

For the second-order corrections we find

$$E^{(2)}_{0,|000\rangle} = 0$$

$$E^{(2)}_{1,|100\rangle} = E^{(2)}_{1,|010\rangle} = \lambda_1 + \lambda_3$$

$$E^{(2)}_{1,|001\rangle} = \lambda_2 + \lambda_3$$

$$E^{(2)}_{2,|011\rangle} = E^{(2)}_{2,|101\rangle} = \lambda_1 + 2\lambda_2 + 4\lambda_3$$

$$E^{(2)}_{2,|110\rangle} = 3\lambda_3$$

$$E^{(2)}_{2,|A\rangle} = \lambda_1 - \lambda_2 + 4\lambda_3$$

$$E^{(2)}_{2,|P\rangle} = \frac{2(p+1)^2\mu}{2\hbar\omega_x + (2p^2-1)\hbar\omega_z} + \frac{3\mu}{2\hbar\omega_x + (6p^2+1)\hbar\omega_z} + \frac{6p^2\mu}{4(p^2+1)\hbar\omega_x + (2p^2-1)\hbar\omega_z}$$

$$E^{(2)}_{2,|Q\rangle} = \frac{2(q+1)^2\mu}{2\hbar\omega_x + (2q^2-1)\hbar\omega_z} + \frac{3\mu}{2\hbar\omega_x + (6q^2+1)\hbar\omega_z} + \frac{6q^2\mu}{4(q^2+1)\hbar\omega_x + (2q^2-1)\hbar\omega_z}$$

with

$$\lambda_1 = \frac{\mu}{\hbar\omega_z} \qquad \lambda_2 = \frac{\mu}{2\hbar\omega_x - \hbar\omega_z} \qquad \lambda_3 = \frac{\mu}{2\hbar\omega_x + \hbar\omega_z} \qquad \mu = -4e^2\epsilon_x^2\epsilon_z.$$

Note added in proof. Klein and Cohen (1991) studied the anharmonicity of hydrogen vibrations and the isotope effect of T_c in PdH with a full-potential LAPW method. Their and our results for vibrational energies coincide well.

References

Blochinzew D I 1985 *Grundlagen der Quantenmechanik* (Thun: Harri Deutsch) (in German)
Carstanjen H D 1989 *Z. Phys. Chem. NF* **165** 141
Christodoulos F and Gillan M J 1991 *J. Phys.: Condens. Matter* **3** 9429
Drexel W, Murani A, Tocchetti D, Kley W, Sosnowska I and Rose D K 1976 *J. Phys. Chem. Solids* **37** 1135
Eckert J, Goldstone J A, Tonks D and Richter D 1983 *Phys. Rev.* B **27** 1980
Elsässer C 1990 *PhD Thesis* Universität Stuttgart (in German)
Elsässer C, Fähnle M, Ho K M and Chan C T 1991a *Physica* B **172** 217
Elsässer C, Ho K M, Chan C T and Fähnle M 1991b *Phys. Rev.* B **44** 10377
Flynn C P and Stoneham A M 1970 *Phys. Rev.* B **1** 3966
Fritzsche A, Hampele M, Herlach D, Maier K, Major J, Schimmele L, Seeger A, Staiger W, Templ W and Baines C 1990 *Hyperfine Int.* **64** 691
Fukai Y and Sugimoto H 1985 *Adv. Phys.* **34** 263
Ho K M, Elsässer C, Chan C T and Fähnle M 1992 *J. Phys.: Condens. Matter* **4** 5189
Ho K M, Tao H J and Zhu X Y 1984 *Phys. Rev. Lett.* **53** 1586
Jena P and Satterthwaite C B (ed) 1983 *Electronic Structure and Properties of Hydrogen in Metals* (New York: Plenum)
Klamt A and Teichler H 1986 *Phys. Status Solidi* b **134** 103, 533
Klein B M and Cohen R E 1991 *Phys. Rev.* B preprint
Kronmüller H, Higelin G, Vargas P and Lässer R 1985 *Z. Phys. Chem. NF* **143** 161
Miller A P and Brockhouse B N 1971 *Can. J. Phys.* **49** 704
Oppeneer P M, Lodder A and Griessen R 1988 *J. Phys. F: Met. Phys.* **18** 1733–43
Puska M J and Nieminen R M 1984 *Phys. Rev.* B **29** 5382
Richter D and Shapiro S M 1980 *Phys. Rev.* B **22** 599
Rose J H, Ferrante J and Smith J R 1981 *Phys. Rev. Lett.* **47** 675
Rowe J M, Rush J J, Smith H G, Mostoller M and Flotow H E 1974 *Phys. Rev. Lett.* **33** 1297
Rush J J, Magerl A, Rowe J M, Harris J M and Provo J L 1981 *Phys. Rev.* B **24** 4903
Rush J J, Rowe J M and Richter D 1984 *Z. Phys.* B **55** 283
Schlapbach L (ed) 1988 *Hydrogen in Intermetallic Compounds I* (Berlin: Springer)
Schober H R and Lottner V 1979 *Z. Phys. Chem. NF* **114** 203
Skoskiewicz T 1972 *Phys. Status Solidi* a **11** K123
Stritzker B and Buckel W 1972 *Z. Phys.* **257** 1
Sugimoto H and Fukai Y 1982 *J. Phys. Soc. Japan* **51** 2554
Tao H J, Ho K M and Zhu X Y 1986 *Phys. Rev.* B **34** 8394
Teichler H 1979 *Z. Phys. Chem. NF* **114** 155
Völkl G and Alefeld J (ed) 1978a *Hydrogen in Metals I* (Berlin: Springer)
—— 1978b *Hydrogen in Metals II* (Berlin: Springer)